Published in final edited form as:
Development. 2008 June ; 135(11): 2043–2053. doi:10.1242/dev.015818.

Progressive myopathy and defects in the maintenance of myotendinous junctions in mice that lack talin 1 in skeletal muscle

Francesco J. Conti[1], **Amanda Felder**[2], **Sue Monkley**[3], **Martin Schwander**[1], **Malcolm R. Wood**[4], **Richard Lieber**[2], **David Critchley**[3], and **Ulrich Müller**[1,*]

1*The Scripps Research Institute, Department of Cell Biology and Institute of Childhood and Neglected Disease, La Jolla, CA*

2 *University of California and Veterans Administrative Centres, Department of Orthopaedics and Bioengineering, San Diego, CA*

3 *University of Leicester, Department of Biochemistry, Leicester, United Kingdom*

4*The Scripps Research Institute, Microscopy Core Facility, La Jolla, CA*

Summary

The development and function of skeletal muscle depend on molecules that connect the muscle fibre cytoskeleton to the extracellular matrix (ECM). β1 integrins are ECM receptors in skeletal muscle, and mutations that affect the α7β1 integrin cause myopathy in humans. In mice, β1 integrins control myoblast fusion, the assembly of the muscle fibre cytoskeleton, and the maintenance of myotendinous junctions (MTJs). The effector molecules that mediate β1 integrin functions in muscle are not known. Previous studies show that talin 1 controls the force-dependent assembly of integrin adhesion complexes and regulates the affinity of integrins for ligands. Here we show that talin 1 is essential in skeletal muscle for the maintenance of integrin attachment sites at MTJs. Mice with a skeletal muscle-specific ablation of the talin 1 gene suffer from a progressive myopathy. Surprisingly, myoblast fusion and the assembly of integrin-containing adhesion complexes at costameres and MTJs advance normally in the mutants. However, with progressive ageing, the muscle fibre cytoskeleton detaches from MTJs. Mechanical measurements on isolated muscles show defects in the ability of talin 1-deficient muscle to generate force. Collectively, our findings show that talin 1 is essential for providing mechanical stability to integrin-dependent adhesion complexes at MTJs, which is crucial for optimal force generation by skeletal muscle.

Keywords

Integrin; talin; muscular dystrophy; myopathy

Introduction

Adhesion of muscle fibres to the ECM is essential for skeletal muscle development and integrity and is mediated by two protein complexes: the dystrophin glycoprotein complex (DGC) and members of the integrin superfamily. The DGC is critical for muscle integrity as exemplified by the fact that mutations in components of the DGC cause muscular dystrophy (Davies and Nowak, 2006; Durbeej and Campbell, 2002; Durbeej et al., 1998; Straub et al., 1997). Far less is known about the function of integrins in muscle. Integrins are heterodimeric

*Corresponding author: Ulrich Müller The Scripps Research Institute Department of Cell Biology 10550 N. Torrey Pines Rd, Mail Drop ICND222 La Jolla, California 92037 P:858−784−7288 umueller@scripps.edu.

ECM receptors consisting of α- and β-subunits (Hynes, 1992). Skeletal muscle fibres in vertebrates express many integrin subunits, including the β1-subunit and its partners α1, α3, α4, α5, α6, α7 and αv (Gullberg et al., 1998). β1 integrins appear to have partially redundant functions in skeletal muscle. Accordingly, inactivation of all α/β1-integrins by CRE/LOX mediated ablation of the β1-subunit gene causes defects in myoblast fusion and sarcomere assembly that are not observed in muscle lacking individual integrin α-subunits (Schwander et al., 2003). Of all integrin α-subunit gene knock-out mice, muscle defects have only been observed for mice with mutations in the integrin α5- and α7-subunit genes, and the phenotypes manifest later than in β1-deficient mice. Chimeric mice that lack the integrin α5β1 in muscle develop dystrophic symptoms (Taverna et al., 1998). Mutations in the gene for the murine integrin α7-subunit cause defects in myotendinous junctions (MTJs) (Mayer et al., 1997) and humans with mutations in the integrin α7-subunit gene suffer from myopathy (Hayashi et al., 1998).

The cytoplasmic domains of integrins bind to many cytoskeletal and signalling proteins (Geiger et al., 2001; Liu et al., 2000), raising questions about the specific contributions of individual proteins to integrin function . Talin 1 is a major integrin effector. It binds to the cytoplasmic domain of several integrin β-subunits and connects β1 integrins at focal adhesions to the actin cytoskeleton (Critchley, 2000). Talin 1 binds to focal adhesion components such as vinculin and focal adhesion kinase (FAK), two important regulators of actin dynamics (Mitra et al., 2005; Ziegler et al., 2006). Importantly, the assembly of focal adhesions is dependent on mechanical force, which regulates recruitment of vinculin to focal adhesions (Balaban et al., 2001; Choquet et al., 1997; Galbraith et al., 2002; Riveline et al., 2001). Talin 1 is critical for force-dependent vinculin recruitment, and for the strengthening of interactions between integrins and cytoskeletal proteins (Giannone et al., 2003). In addition, in vitro and in vivo studies have shown that talin 1 modulates the ligand binding activity of the extracellular domain of integrins by a mechanisms termed insight-out signalling (Calderwood, 2004a; Campbell and Ginsberg, 2004; Nieswandt et al., 2007; Petrich et al., 2007).

In skeletal muscle fibres, talin 1 is localized to costameres and MTJs (Tidball et al., 1986), and its expression is regulated by mechanical loading (Frenette and Tidball, 1998). However, the function of talin 1 in vertebrate muscle is unclear since mice with a mutation in the talin 1 (*Tln1*) gene die during gastrulation (Monkley et al., 2000). Vertebrates contain a second talin gene (*Tln2*) encoding talin 2 (McCann and Craig, 1997; McCann and Craig, 1999; Monkley et al., 2001), whose function in skeletal muscle is likewise not known. Studies with myoblasts in culture show that expression of talin 2 is upregulated in myotubes, while talin 1 expression remains unchanged during differentiation (Senetar et al., 2007). The genomes of *C. elegans* and *D. melanogaster* contain only one talin gene, which is essential for the attachment of muscle fibers to surrounding tissue (Brown et al., 2002; Cram et al., 2003). The invertebrate ortholog of the vertebrate integrin β1-subunit gene plays a similar role, indicating that talin 1 mediates integrin functions in invertebrate muscle (Brabant et al., 1996; Brown, 1994; Brown et al., 2002; Cram et al., 2003; Gettner et al., 1995; Lee et al., 2001; Leptin et al., 1989; Volk et al., 1990). However, the mechanism by which defects in talin lead to the perturbation of adhesion sites is unclear.

To define the function of talin 1 in skeletal muscle of vertebrates, we have taken a genetic approach and crossed mice carrying a floxed *Tln1* allele with mice expressing CRE in developing skeletal muscle. We show here that talin 1 is not essential for the assembly of integrin β1-dependent adhesion complexes at costameres and MTJs. Instead, talin 1 plays an important role in stabilizing adhesion complexes at MTJs, thereby providing resistance against mechanical stress that is exerted during muscle contraction and relaxation. Surprisingly, while talin 2 is abundantly expressed in skeletal muscle, it cannot compensate for loss of talin 1, suggesting that the two talin isoforms are not entirely functionally interchangeable.

Materials and Methods

Mouse lines and genotyping

The generation of *Tln1-flox* mice and *HSA-CRE* mice have been described (Leu et al., 2003; Nieswandt et al., 2007; Petrich et al., 2007; Schwander et al., 2003). The mice were on a mixed 129xC57Bl/6 genetic background. For genotyping, tail DNA was analyzed by PCR using primers for *Tln1* as indicated in Fig. 1: 5'AAGCAGGAACAAAAGTAGG TCTCC3'; (b) 5'GCATCGTCTTCACCACATTCC3'; (c) 5'TAGAGAAGGTTCAGC TGTCAGGG3'.

Real time PCR

Transcript levels for talin 1 and talin 2 were determined by quantitative real-time PCR (RT-PCR). RNA from gastrocnemius muscle from 5 days (n=3) and 6-months (n=3) old C57Bl/6 mice was prepared using Trizol LS (Invitrogen). 1.6−2 μg RNA was reverse transcribed using the Superscript III System (Invitrogen). Transcripts were quantitated by RT-PCR using Chromo4 (MJ Research) and SYBR GREEN (Applied Biosystems). Two sets of primers were used for each transcript (Talin 1: Set 1: 5'GGAAATCTGCCGGA GTTTGG3'; 5'TTGGCTGTTGGGGTCAGAGA3'; Set 2: 5'GGGCTGGAGGGAGATG AAGA3'; 5'AGAGCCGTGCTCCACTTTCC3'; Talin 2: Set 1 5'AAAACCCGAATG AGCCTGTGA3'; 5'GAAATCCCTGCCATTGACTCG3'; Set 2 5'GAAAACCCGAAT GAGCCTGTG3'; 5'GAAATCCCTGCCATTGACTCG3'). Primers spanned at least one exon/intron boundary and were verified in BLAST searches for specificity. To determine primer efficiency, RNA was diluted serially and linear regression analysis was applied. The slope of the resulting curve was used as a measure of PCR efficiency ($E=(10^{-1/\text{slope}})-1$). Efficiencies of the primer pairs were 95% − 98%. Both set of primers produced comparable results and data from one set are shown. mRNA levels were determined using the comparative threshold (Ct) method (Livak and Schmittgen, 2001) and normalised to glyceraldehyde-3-phosphate dehydrogenase or β-actin mRNA.

Antibodies, immunohistochemistry, and electron microscopy

Rabbit antibodies to talin 1 and talin 2 were produced at Animal Pharm Services (Healdsburg) using peptides corresponding to amino acids 1830−1850 (mouse talin 1) and 940−957 (mouse talin 2). Immunohistochemistry was carried out as described (Schwander et al., 2003) using the following antibodies: mouse monoclonal antibodies against vinculin (Sigma), dystrophin (clone NCL-DYS2, Novocastra), MHCf (Sigma) and ILK (Li et al., 1999); rabbit polyclonal antibodies against collagen IV (Chemicon), laminin (Chemicon), talin 1, talin 2 and α7-integrin (kindly provided by U. Meyer). Electron microscopy was carried out as described (Schwander et al., 2003).

Western blotting

Gastrocnemius muscles were lysed in 1% TX100/PBS supplemented with protease inhibitor cocktail (Roche Diagnostics). Equal amounts of protein as determined using the Micro BCA^{tm} Kit (Pierce) were analyzed by western blotting with the following antibodies: talin 1, vinculin (Sigma), ERK 1/2 total and phosphorylated (Cell Signaling Technology, Danvers, MA), FAK and FAK-PY^{397} (UBI). To verify equal loading, membranes were stripped with stripping solution (Chemicon) and probed with antibodies to α-tubulin (Sigma). Signal intensity was determined by denisitometry using MetaMorph Optical Density analysis software (Molecular Devices Inc.). Films from 3 independent experiments were scanned.

Evans blue dye (EBD) uptake and creatine kinase (CK) assay

EBD (Sigma) was dissolved in PBS (10 mg/ml), and injected via the tail vein with 50 μl solution per 10 g body weight. After 5 h, mice were sacrificed, muscles were dissected and visually

inspected. Tissues were fixed over night with 4% PFA. 12 μm sections of gastrocnemius and diaphragm muscles were analyzed using an Olympus BX50WI epifluorescence microscope. Measurements of creatine kinase (CK) levels from blood samples of 6−7 months old mice were performed by Antech Diagnostics (Irvine, CA). To evaluate EBD uptake after exercise, 5 months old *Tln1HSA-CREko* and wild-type mice (4−5 per genotype) were injected with and EBD solution and 1 h later subjected to exercise. Mice were allowed to warm up by running at 10 meter/min on a 0° incline for 5 min. After 5 min rest, mice were run at 17m/min on a 0° incline for 30 min. Animals were returned to their cages and sacrificed 24 h after exercise, muscles were dissected and EBD incorporation evaluated as described above.

Cardiotoxin experiments

50 μl of 10 μM cardiotoxin (Sigma-Aldrich) were injected in the calf muscles of 8−12 weeks old mice mice. The controlateral leg was injected with 50 μl PBS as a control. Muscles were isolated at 5, 10 and 21 days following injection, fixed with 4% paraformaldehyde, and embedded in paraffin. Sections were prepared and stained with hematoxylin and eosin and morphology of myofibres evaluated for regeneration.

Isometric and eccentric contraction cycles

Mice were sacrificed and the 5th EDL (extensor digitorum longus) muscle was dissected in Ringer's solution (137 mM NaCl, 5 mM KCl, 1 mM NaH_2PO_4, 24 mM $NaHCO_3$, 2 mM $CaCl_2$, 1 mM $MgSO_4$, 11 mM glucose, 10 mg/l curare). Using 8−0 silk sutures, the muscle origin was secured by the tendon at a rigid post and the insertion was secured by the tendon to the arm of a dual-mode ergometer (model 300B, Aurora Scientific). Muscle was bathed in Ringer's solution, which was determined to be 10 °C during measurements. Muscle length (ML) was measured, increased by 10%, and sarcomere length was measured by laser diffraction at 632.8 nm and adjusted to 3.0 μm. The EDL muscle was subjected to three passive stretches, one every 3 min, each time stretched 10% of ML at the velocity of 0.7 ML/sec. Maximum isometric tension was measured by applying a 400 msec train of 0.3 msec pulses delivered at 100 Hz while muscle length was maintained constant. This measurement was repeated again after 5 min. The stimulation frequency chosen for these isometric contractions and the other contractions that follow was 100 Hz, as this frequency produced a fused tetanic contraction, but was low enough to prevent excessive fatigue. Each muscle underwent 10 eccentric contractions (EC), one every 3 min, each time stretched to 15% of ML at the velocity of 2 ML/sec. Following the EC cycle, the muscle length was returned to its initial value and post-eccentric isometric tension was measured by applying a 400 msec train of 0.3 msec pulses, delivered at 100 Hz while muscle length was maintained constant. This measurement was repeated 2 times, at 5 min intervals. Muscle weight was measured to determine the physiological cross-sectional area (Sam et al., 2000). Data was acquired using a CA-1000 data board and analyzed in LabVIEW 7.0 (National Instruments, Austin, TX).

Results

Skeletal muscle specific *Tln1* knock-out mice

To study the function of talin 1 in skeletal muscle, we have employed a conditional knockout approach using the CRE/LOX system. A gene-targeting vector was generated in which exons 2−5 (of which exon 2 is the first coding exon) of the *Tln1* gene were flanked by loxP sites (Fig. 1A). A selection cassette containing a *neomycin* gene and a third loxP site was introduced upstream of the first loxP site. Mice were generated that transmitted the targeted allele through the germline. These mice were crossed with a CRE deleter mouse (Schwenk et al., 1995). Mice with different recombination events were recovered. In one line only the *neomycin* cassette was lost, maintaining floxed exons 1−4 (referred to as conditional allele, $Tln1^{flox}$); 2). In a second line, the floxed region including the *neomycin* cassette and exons 1−4 were removed

(referred to as deleted allele, *Tln1*$^{-}$) (Fig. 1A). *Tln1*$^{flox/flox}$ mice showed no overt abnormality, demonstrating that the presence of loxP sites did not affect *Tln1* function (data not shown). *Tln1*$^{-/-}$ died at gastrulation (6.5−7.5 days post-coitum) (data not shown), thus phenocopying mice in which the *Tln1* allele has been ablated (Monkley et al., 2000).

To abolish talin 1 expression in skeletal muscle, we took advantage of mice that express CRE under control of the human skeletal α-actin (HSA) promoter (*HSA-CRE*) (Leu et al., 2003; Schwander et al., 2003). We have previously shown that the *HSA-CRE* transgene is expressed as early as embryonic day (E) 9.5 in somites, and throughout all muscle groups by E14.5 (Schwander et al., 2003). *Tln1*$^{flox/flox}$ were mated with *Tln1*$^{flox/+}$ mice that also contained a *HSA-CRE* transgene (*Tln1*$^{flox//+}$ *HSA-CRE*$^{+/-}$) to obtain mutant (*HSA-CRE*$^{+/-}$ *Tln1*$^{flox/flox}$, referred to as *Tln1HSA-CREko* mice) and control (*HSA-CRE*$^{-/-}$ *Tln*$^{flox/flox}$ or *HSA-CRE*$^{-/-}$ *Tln*$^{flox/+}$ referred to as wild-type because their phenotype was indistinguishable from C57Bl/6 mice) offspring. To confirm recombination of the *Tln1*^{flox} allele in *Tln1HSA-CREko* mice, we performed PCR analysis of DNA extracted from skeletal muscle of E14.5 and postnatal day (P) 2 mice; *Tln1*$^{flox/flox}$ and *Tln1*$^{flox/f+}$ mice that lacked the *HSA-CRE* transgene were analyzed in parallel as controls. A 707 bp band corresponding to the recombined *Tln1*^{flox} allele was detected in skeletal muscle of *Tln1HSA-CREko* mice as early as E14.5 (Fig. 1B), but not in non-muscle tissue (data not shown) or control mice (Fig. 1B).

Talin 1 expression is abolished in skeletal muscle

To confirm that we had inactivated *Tln1* in *Tln1HSA-CREko* mice, we raised in rabbits antibodies that are specific for talin 1 and for talin 2 (see Material and Methods) and analyzed protein expression in muscles including gastrocnemius, tibialis and diaphragm. At late embryonic and early postnatal ages when skeletal muscle fibres are actively forming, talin 1 expression was detected at the sarcolemma of wild-type mice but not in the mutants (Fig. 2A,B, arrows). Some cells in the mutants expressed talin 1 (Fig. 2A,B arrowheads), but we identified them by morphology and costaining with antibodies to VE-cadherin as endothelial cells (Fig, 2E). Similarly, in muscle from 6 months old mice, talin 1 expression was not detectable in muscle fibres (Fig. 2C,D) and only persisted in blood vessels (Fig. 2D, arrowhead). Western blot analysis carried out with extracts obtained from skeletal muscle of P2 and P8 *Tln1HSA-CREko* mice further confirmed that talin 1 expression was essential abolished (Fig. 2F). Residual expression was likely due to talin 1 expressed in blood vessels. In addition, we detected talin 2 expression by Western blot (Fig. 2F) and immunohistochemistry (Fig. 6M,N), but we failed to detect compensatory talin 2 upregulation upon removal of talin 1 (Fig. 2F, Fig. 6M,N).

The expression levels of the *Tln1* and *Tln2* transcripts in gastrocnemius muscle were also determined by real-time PCR. Expression levels for *Tln2* were 4−5 fold higher than for *Tln1* in both 5 days (*Tln1*=1.03 ± 0.16; *Tln2*=4.70 ± 0.44; p=0.004) and 6 months old muscle (*Tln1*=1.00 ± 0.06; *Tln2*=4.1 ± 0.31; p=0.002) (Fig. 2 G). This analysis corroborates earlier findings, which indicate that *Tln2* mRNA is the predominant isoform expressed in skeletal muscle (Monkley et al., 2001;Senetar et al., 2007).

Progressive accumulation of dysmorphic muscle fibres in *Tln1HSA-CREko* mice

Tln1HSA-CREko mice were born at the expected Mendelian ratio, were viable and fertile, were in appearance indistinguishable from wild-type littermates (data not shown), and grew at normal rates (Fig. 2H). However, histological examination revealed progressive defects in muscle fibre morphology. We analyzed several muscle groups including gastrocnemius, soleus, and diaphragm collected from animals between P15 and 6 months. At P15 and P60, all muscle groups appeared normal (Fig. 3A-H; data not shown); wild-type and *Tln1*-deficient muscle fibres were regular in diameter. Morphological defects were obvious in muscle of

Tln1-deficient mice by 6 months of age, and were more commonly observed in the diaphragm. In contrast to wild-type mice (Fig. 3I,K) muscle fibres in diaphragm muscle of mutant animals appeared less regular in diameter, with enlarged (Fig. 3J,L) and distorted (Fig. 3M) fibres. Dysmorphic fibres were also evident close to the MTJs of diaphragm muscle (Fig. 3O,P). Centrally located nuclei and an accumulation of interstitial cells were occasionally detectable. However, unlike the situation in mice lacking expression of the integrin α7-subunit (Mayer et al., 1997), a diffuse centronuclear myopathy was not observed.

Integrins and talin 1 have been implicated in myoblast proliferation and differentiation (Senetar et al., 2007). In postnatal muscle, non-proliferating myoblasts are localized between myofibres and the basal lamina, where they constitute the satellite cell population. Upon muscle injury, satellite cells proliferate, fuse and regenerate new myofibres, which are characterised by variable size and centrally located nuclei (Shi and Garry, 2006). To evaluate whether absence of a centronuclear myopathy was caused by defects in satellite cell function, we injected gastrocnemius muscles of 2 months old mice with cardiotoxin and analyzed muscle fiber morphology 5, 10 and 21 days later. At all time points *Tln1HSA-CREko* and wild-type mice presented signs of effective muscle regeneration. Five days after toxin injection, necrotic fibres and small fibres with centrally located nuclei, indicative of regenerating fibres, were evident and immune cell infiltrate was noted (Supp. Fig. 1A-D). After 10 days, affected fibres presented with central located nuclei, but muscle architecture was largely restored (Supp. Fig. 1E,F). By 21 days, regeneration was complete (Supp. Fig. 1 G,H; data not shown). We conclude that the absence of a centronuclear myopathy in *Tln1HSA-CREko* mice is not caused by an impaired capacity of mutant muscle to regenerate.

Talin 1 is not essential to maintain sarcolemmal integrity

An increase in fragility of the sarcolemma is observed in several forms of muscular dystrophy (Carpenter and Karpati, 1979; Schmalbruch, 1975; Straub et al., 1997; Weller et al., 1990). To evaluate damage to the sarcolemma, Evans Blue dye (EBD) was injected in 6 months old *Tln1HSA-CREko* and wild-type mice, and muscles were dissected after 5 hours to evaluate dye incorporation. While connective tissue presented a blue coloration, muscles including the diaphragm (Fig. 3Q,R), gastrocnemius and soleus (Fig. 3S,T; data not shown) failed to accumulate EBD. Occasionally, few EBD-stained fibres were evident, independently of the genotype of the mice (Fig. 3J, arrow). Histologically these EBD-positive fibres appeared damaged, possibly in response to normal muscle usage. This, together with the positive coloration of interstitial tissue, validated successful circulation of the dye. EBD-positive fibres in damaged muscle appeared fluorescent by light microscopy (Fig. 3T). In both wild-type and *Tln1*-deficient muscle, fluorescence was only observed in tendons and interstitial tissue, and not in muscle fibres (Fig. 3R,S).

A more sensitive indication of membrane integrity is gained by evaluating the efflux of intracellular proteins from damaged muscle fibres (Rosalki, 1989). In 6 months old *Tln1HSA-CREko* mice, serum creatine kinase was elevated ~3-fold compared to wild-type mice (1526.20 ±151.44 U/l and 593.85±154.23 U/l, respectively) (Fig. 3Y). This increase is mild when compared to other mouse models of muscular dystrophy (Sonnemann et al., 2006).

Finally, we evaluated whether talin 1-deficient muscles were more susceptible to muscle fiber damage when subjected to exercise as observed in other models for muscular dystrophy (Armstrong et al., 1983; Hamer et al., 2002; McNeil and Khakee, 1992; Vilquin et al., 1998). EBD was injected in 5−6 month old mice and, 1 hour after injection, mice were run on a treadmill for 30 minutes. No major dye incorporation was observed in diaphragm and gastrocnemius muscle from wild-type mice (n=4) (Supp. Fig. 2A,C,F) and in *Tln1HSA-CREko* mice (n=4) (Supp Fig. 2B, D). Mild EBD accumulation was only observed in one gastrocnemius muscle in one mutant mice (Supp. Fig. 1E), and in the paraspinalis muscles in

a second mouse (Supp. Fig. 1G), but the damage was mild in comparison with what has been observed in mice carrying mutations affecting DGC proteins (Sonnemann et al., 2006).

Collectively, these data suggest that sarcolemmal integrity is mildly defective when the function of talin 1 is perturbed. Mild damage to the sarcolemma was also observed in patients and mice with mutations in the gene for the integrin α7-subunit (Hayashi et al., 1998; Rooney et al., 2006).

Talin1 is not essential for the assembly of integrin complexes at costameres

Talin binds to proteins that are localized to costameres, including β1 integrins, vinculin, actin and FAK (Critchley, 2000). Since defects in muscle fibre morphology could result from altered assembly of costameres, we assessed whether talin 1 ablation impaired costamere assembly *in vivo*. We analyzed the distribution of costameric proteins in 6-months old mice by immunohistochemistry, but observed no obvious defects. β1 integrins and α-actinin were normally localized, forming a regular array (Fig. 4 A-D). Talin 1 directly binds to vinculin, but vinculin was still localized to costameres in *Tln1*-deficient skeletal muscle fibres (Fig. 4 E, F). Consistent with the lack of extensive sarcolemmal damage (Fig. 3), localization of dystrophin was also unaffected (Fig. 4 G, H). Morphological defects of muscle fibres could be caused by defects in the basement membrane around muscle fibres, but no obvious defects were apparent in the localization of collagen type IV and laminin (Fig. 4 I-L). Sarcomere integrity was also evaluated by electron microscopy (EM). In both wild-type and *Tln1*-deficient skeletal muscle fibres, the sarcomeres were well organised, with evident Z- lines in both 1-month (Fig. 4 M, N) and 6-months old (Fig. 4 O, P) mice. In *Tln1*-deficient muscle fibres, the sarcomeres occasionally appeared hypercontracted and M-bands were not always evident; the Z-line, which includes β1-integrin-containing complexes and corresponds to costameres, was always visible (Fig. 4 O, P).

Talin 1 directly associates with FAK (Chen et al., 1995). Integrin binding to ECM ligands leads to activation of FAK by autophosphorylation at Tyr^{397}, creating a binding site for Src, which phosphorylates focal adhesion components and activates MAPK signalling (Mitra et al., 2005). In *Tln1HSA-CREko* mice, expression levels and phosphorylation of FAK at Tyr^{397} were comparable to wild-type mice (Fig. 5A,D). Phosphorylation levels of ERK 1/2 were also normal (Fig. 5B,D). Finally, Western blot analysis with antibodies to vinculin and the integrin β1-subunit reveal that expression levels of these proteins were not changed in muscle from *Tln1HSA-CREko* mice (Fig. 5C,D). Taken together, these data indicate that loss of talin 1 in skeletal muscle does not lead to major defects in the assembly of costameres, or in FAK and MAPK signalling.

Talin 1 is essential for the maintenance of the connection between integrins and myofilaments at MTJs

Alterations in muscle fibre morphology could result from defects at MTJs. Ultrastructural analysis showed that the structure of the lamina densa at MTJs, which is absent in mice with genetic ablation of β1-integrins and altered in α7-integrin mutants (Miosge et al., 1999; Schwander et al., 2003), was still visible in *Tln1HSA-CREko* mice (Fig. 6A, B). Immunostaining of sections f0rom 6 months old mice demonstrated that the distribution of collagen IV and laminin was normal at MTJs in mutant animals (Fig. 6C-F). In addition, α7-integrin, vinculin and integrin linked kinase (ILK) localized at the MTJ, suggesting that the integrin complexes at MTJs assemble in the absence of talin 1 and are largely functional to mediate adhesive interactions (Fig. 7G-L). We also observed that talin 2 is localized at the MTJs without any obvious up-regulation in the mutants (Fig. 7M, N). Taken together, these data provide strong evidence that integrin-dependent adhesion complexes still form at MTJs in the absence of talin 1.

Further ultrastructural analysis of skeletal muscle in 1-month and 6-months old animals revealed that the attachment of myofilaments at MTJ progressively failed in *Tln1HSA-CREko* mice. At the MTJs of wild-type mice, the sarcolemma was extensively folded (Fig. 7A, D). Myofilaments displayed a regular sarcomeric structure, and were connected to the subsarcolemmal electron dense plaque at the basement membrane (Fig. 7A,D,F; arrowheads). In *Tln1HSA-CREko* mice, myofilaments failed to connect to the basement membrane and were retracted (Fig. 7C,E,G). Necrotic material accumulated between the myofilaments and the basement membrane (Fig. 7C,E,G; asterisks) and included vacuoles and membranous debris. The subsarcolemmal plaque was present in *Tln1HSA-CREko* mice, but its thickness was reduced and, in particular, it was discontinuous in areas were myofilaments failed to attach (arrows in Fig. 7G). The interdigitations of muscle fibres with the tendon were also perturbed (Fig. 7C,E,G). Defects were noted in different muscles, including tibialis (Fig. 7A-C), diaphragm (Fig. 7D-G) and gastrocnemius (not shown). Ultrastructural analysis of extrajunctional areas revealed additional abnormalities, which are commonly observed in dystrophic muscles, including the presence of structures that resembled vacuoles (Fig. 7E,G,I,J), suggesting some degree of degeneration. Upon closer inspection, some vacuoles could be identified as morphologically abnormal mitochondria (data not shown). Likely, these were not artefacts of sample preparation, since normal and abnormal mitochondria were found closely juxtaposed to each other (white arrows in Fig 7I). In some areas, excessive accumulation of mitochondria was noted (Fig. 7K, L).

Collectively, our finding show that in the absence of talin 1, integrin adhesion complexes still form at MTJs and connect to the muscle fibre cytoskeleton. However, with progressive age, myofilaments detach, suggesting that talin 1 is required for maintaining their interaction with integrin adhesion complexes during mechanical strain.

Altered mechanical properties of skeletal muscle fibres in *Tln1HSA-CREko* mice

Defects in MTJs are likely to affect the ability of skeletal muscle fibres to generate force and to resist mechanical damage during contraction. To test this hypothesis, we applied defined length changes to muscles using an ex vivo experimental setup. The 5th toe extensor digitorum longus (EDL) muscle was isolated from 2−3 months old and 6−7 months old mice and subjected to cyclic isometric or eccentric contractions. Isometric contractions are performed by stimulating muscle fibers to contract while keeping the length of the muscle constant, and provide a measure of the force the muscle is able to exert (Fig. 8B). Eccentric contractions are performed by lengthening the muscle while at the same time stimulating contraction (Fig. 8C) and induce damage in muscle fibres (Armstrong et al., 1983;Lieber et al., 1991). The difference in isometric stress produced by muscle fibers before and after the eccentric contraction cycle provides a measure of susceptibility to mechanical damage (Sam et al., 2000). No significant difference was observed in the length and mass of isolated wild-type and *Tln1*-deficient muscles (Fig. 8A), and all force values were normalised against the physiological cross-sectional area (Fig. 8A), which takes into account differences in muscle mass, length and in the orientation of muscle fibres (see Materials and Methods). At 2−3-months of age, the isometric stresses produced by *Tln1*-deficient muscle fibres was comparable to wild-type muscle fibres ($p=0.413$ pre-eccentric, $p=0.892$ post-eccentric) (Fig. 8 D). In contrast, force production was markedly impaired in muscle obtained from 6−7-month old *Tln1HSA-CREko* mice (Fig. 8E). In an eccentric contraction cycle, mutant mice show a significant reduction in maximum pre-eccentric ($p=0.0276$) and post-eccentric ($p=0.0358$) isometric stress (Fig. 8F,G). Additionally, for older *Tln1*-deficient muscles, the peak stresses exerted during the eccentric contraction were significantly reduced from wild-type values in every eccentric contraction except the initial one, which showed greater variability (Supp Fig. 3B). Similarly, the work performed on the muscle normalized by muscle mass was decreased in the 6−7 months old *Tln1HSA-CREko* mice for each eccentric contraction when compared to wild-type (Supp.

Fig. 3D). Values of peak stress and work were not significantly different between the muscles obtained from 2-months old wild-type and mutant mice (Supp. Fig. 3A,C). The forces generated by wild-type and mutant fibres decreased during the eccentric contraction protocol (Fig. 8D,F). At both 2-months and 7-months, the force drop was comparable between wild-type and *Tln1*-deficient muscles (Fig. 8 H). However, since 7-months old mutant muscles exerted considerably less force during the contraction protocol, reduced damage and fatigue and consequently a smaller force drop were expected. The greater than expected force drop in mutant muscle suggests that *Tln1*-deficient muscle was susceptible to eccentric-contraction induced damage. These data are consistent with a failure of the attachment of skeletal muscle fibres at MTJs. Overall, we conclude that ablation of talin 1 causes a progressive impairment of the capacity of muscle to generate and to bear force.

Discussion

We show here that talin 1 is critical for the maintenance of integrin attachment sites at MTJs. *Tln1HSA-CREko* mice were viable and fertile, but suffered from a progressive myopathy. While integrins and some of their effectors such as FAK, ILK, and vinculin still were localized to muscle attachment sites at costameres and MTJs, MTJs showed structural abnormalities. Defects in the ultrastructure of MTJs, such as decreased interdigitations of muscle and tendon and retraction of myofilaments from electron-dense plaques at the plasma membrane, indicate that in the absence of talin 1 the mechanical connection of actin filaments and integrins at the MTJ was compromised. In contrast, sarcolemmal integrity was largely maintained. Defects in skeletal muscle where prominent in 6−7 months old mice, and were only occasionally noted in 1−2 months old animals, suggesting that the defects were caused by mechanical failure of MTJs under duress. In agreement with this finding, isolated muscle fibers from 7-months but not 2-months were severely compromised in their ability to generate force.

Previous studies have shown that in invertebrates talin is essential to mediate interactions between integrins and the muscle fibre cytoskeleton (Brown et al., 2002; Cram et al., 2003), but the mechanism of talin function has remained unclear. By taking advantage of a vertebrate model system that provides greater access to study the biophysical properties of muscle, we now provide evidence that talin 1 has an important biomechanical role in muscle. Studies with cells in culture have shown that talin 1 localizes to focal adhesions where it interacts with β1 integrins, FAK, vinculin and actin (Borowsky and Hynes, 1998; Critchley, 2000), and with layilin in membrane ruffles (Borowsky and Hynes, 1998). The assembly of adhesion complexes at focal adhesions is controlled by mechanical force. Forces that are applied to nascent integrin adhesion sites induce a strengthening of the integrin-cytoskeleton interaction, initiating focal adhesion formation and promoting maturation (Balaban et al., 2001; Choquet et al., 1997; Galbraith et al., 2002; Riveline et al., 2001). Mechanical force accelerates the localization of vinculin to focal adhesions, which depends on talin 1 (Giannone et al., 2003). Our findings now show an important mechanical function for talin 1 in vertebrate skeletal muscle in vivo. At MTJs, integrin adhesion complexes containing the integrin α7- and β1-subunits, ILK, and vinculin assembled in the absence of talin 1. However, talin 1-deficient MTJs showed greater susceptibility to mechanical stress-induced damage. MTJs in muscle such as diaphragm that are under constant workload showed the most prominent defects. Mechanical measurements on isolated muscle fibres demonstrated that talin 1-deficient fibres generated less force than wild-type muscle fibres. MTJs in *Tln1HSA-CREko* mice still contained talin 2 but were unstable, suggesting that talin 1 and talin 2 are not entirely functionally interchangeable.

Previous studies have shown that talin 1 is of central importance for integrin function, regulating interactions of the β1 integrin with the cytoskeleton and with ECM ligands (Calderwood, 2004b; Campbell and Ginsberg, 2004; Ginsberg et al., 2005; Nieswandt et al., 2007; Petrich et al., 2007). Ablation of the gene encoding the integrin β1 subunit during skeletal

muscle development leads to defects in myoblast fusion and sarcomere assembly (Schwander et al., 2003). We were surprised that we did not observe similar defects in *Tln1HSA-CREko* mice. The migration and fusion of myoblasts was not obviously perturbed, and immunohistochemical and ultrastructural analysis revealed no defects in the assembly of costameres and integrin complexes. How can these findings be reconciled? Talin 1 may still have essential functions early in skeletal muscle development, for example in myoblast migration, that have escaped detection since gene-inactivation using HSA-CRE may have been incomplete at early ages. Furthermore, talin 2 may compensate for some talin 1 functions. In agreement with previous findings (Monkley et al., 2001; Senetar and McCann, 2005; Senetar et al., 2007) we observed prominent talin 2 expression in skeletal muscle. However, our findings as well as previous studies suggest that talin 2 and talin 1 are not entirely interchangable. First, genes for talin 1 and talin 2 have been identified in all available vertebrate genomes, indicating that evolutionary pressure has maintained two talin genes. Second, *Tln1-null* mice are embryonically lethal (Monkley et al., 2000) indicating that *Tln2* cannot compensate for *Tln1* in early mouse development. Third, while talin 1 and 2 share a high degree of identity, amino acid differences in functionally important domains such as FERM and I/LWEQ (actin-binding) domains have been maintained throughout evolution (Senetar and McCann, 2005). These differences may confer specific functions to each protein. Consistent with this interpretation, talin 1 and 2 have different affinity of F-actin (Senetar et al., 2004). Fourth, talin 1 and talin2 have distinct binding partners in skeletal muscle (Senetar and McCann, 2005). Finally, the two-piconewton slip bond between fibronectin and the cytoskeleton depends on talin 1. Talin 2 cannot compensate for the function of talin 1 in this process (Jiang et al., 2003). The latter finding suggests that talin 1 has a specialized function in force coupling, which could be especially important in maintaining MTJs under mechanical duress. Talin 2 likely sufficient for the assembly of integrin adhesion complexes at MTJs, but in the absence of talin 1, MTJs progressively fail.

Our data suggest that the functions of talin 1 in the regulation of integrin activation may be tissue-specific. Unlike the situation in megakaryocytes and platelets, where a rapid and discrete modulation of integrin affinity for the ECM is required for proper function (Calderwood, 2004a; Campbell and Ginsberg, 2004; Nieswandt et al., 2007; Petrich et al., 2007), affinity modulation may be less crucial at more stable adhesion complexes at MTJs. Importantly, integrin activation by talin was evaluated only for the integrin β1A splice variant, while adult skeletal muscle expresses integrin-β1D, which provides a stronger mechanical link to the actin cytoskeleton.

Finally, our findings have implications for understanding disease mechanisms. Mutations that affect talin 1 and the integrin α7β1 cause fragility of MTJs, but membrane damage is mild (Hayashi et al., 1998; Mayer et al., 1997). In contrast, MTJs are maintained when the DGC is affected, but plasma membrane damage is prominent (Straub et al., 1997). Collectively, these findings suggest that ECM receptors of the integrin family and their effectors control MTJ stability, while the DGC has a major function in maintaining integrity of the sarcolemma.

Acknowledgements

We thank Ulrike Mayer (University of East Anglia) and Cary Wu (University of Pittsburgh) for generously providing us with antibodies to the integrin α7 subunit and ILK, respectively. This research was funded with support from the National Institute of Health (U.M., NS046456).

References

Armstrong RB, Ogilvie RW, Schwane JA. Eccentric exercise-induced injury to rat skeletal muscle. J Appl Physiol 1983;54:80–93. [PubMed: 6826426]

Balaban NQ, Schwarz US, Riveline D, Goichberg P, Tzur G, Sabanay I, Mahalu D, Safran S, Bershadsky A, Addadi L, et al. Force and focal adhesion assembly: a close relationship studied using elastic micropatterned substrates. Nat Cell Biol 2001;3:466–72. [PubMed: 11331874]

Borowsky ML, Hynes RO. Layilin, a novel talin-binding transmembrane protein homologous with C-type lectins, is localized in membrane ruffles. J Cell Biol 1998;143:429–42. [PubMed: 9786953]

Brabant MC, Fristrom D, Bunch TA, Brower DL. Distinct spatial and temporal functions for PS integrins during Drosophila wing morphogenesis. Development 1996;122:3307–17. [PubMed: 8898242]

Brown NH. Null mutations in the alpha PS2 and beta PS integrin subunit genes have distinct phenotypes. Development 1994;120:1221–31. [PubMed: 8026331]

Brown NH, Gregory SL, Rickoll WL, Fessler LI, Prout M, White RA, Fristrom JW. Talin is essential for integrin function in Drosophila. Dev Cell 2002;3:569–79. [PubMed: 12408808]

Calderwood DA. Integrin activation. J Cell Sci 2004a;117:657–66. [PubMed: 14754902]

Calderwood DA. Talin controls integrin activation. Biochem Soc Trans 2004b;32:434–7. [PubMed: 15157154]

Campbell ID, Ginsberg MH. The talin-tail interaction places integrin activation on FERM ground. Trends Biochem Sci 2004;29:429–35. [PubMed: 15362227]

Carpenter S, Karpati G. Duchenne muscular dystrophy: plasma membrane loss initiates muscle cell necrosis unless it is repaired. Brain 1979;102:147–61. [PubMed: 427527]

Chen HC, Appeddu PA, Parsons JT, Hildebrand JD, Schaller MD, Guan JL. Interaction of focal adhesion kinase with cytoskeletal protein talin. J Biol Chem 1995;270:16995–9. [PubMed: 7622520]

Choquet D, Felsenfeld DP, Sheetz MP. Extracellular matrix rigidity causes strengthening of integrin-cytoskeleton linkages. Cell 1997;88:39–48. [PubMed: 9019403]

Cram EJ, Clark SG, Schwarzbauer JE. Talin loss-of-function uncovers roles in cell contractility and migration in C. elegans. J Cell Sci 2003;116:3871–8. [PubMed: 12915588]

Critchley DR. Focal adhesions - the cytoskeletal connection. Curr Opin Cell Biol 2000;12:133–9. [PubMed: 10679361]

Davies KE, Nowak KJ. Molecular mechanisms of muscular dystrophies: old and new players. Nat Rev Mol Cell Biol 2006;7:762–73. [PubMed: 16971897]

Durbeej M, Campbell KP. Muscular dystrophies involving the dystrophin-glycoprotein complex: an overview of current mouse models. Curr Opin Genet Dev 2002;12:349–61. [PubMed: 12076680]

Durbeej M, Henry MD, Campbell KP. Dystroglycan in development and disease. Curr Opin Cell Biol 1998;10:594–601. [PubMed: 9818169]

Frenette J, Tidball JG. Mechanical loading regulates expression of talin and its mRNA, which are concentrated at myotendinous junctions. Am J Physiol 1998;275:C818–25. [PubMed: 9730966]

Galbraith CG, Yamada KM, Sheetz MP. The relationship between force and focal complex development. J Cell Biol 2002;159:695–705. [PubMed: 12446745]

Geiger B, Bershadsky A, Pankov R, Yamada KM. Transmembrane crosstalk between the extracellular matrix--cytoskeleton crosstalk. Nat Rev Mol Cell Biol 2001;2:793–805. [PubMed: 11715046]

Gettner SN, Kenyon C, Reichardt LF. Characterization of beta pat-3 heterodimers, a family of essential integrin receptors in C. elegans. J Cell Biol 1995;129:1127–41. [PubMed: 7744961]

Giannone G, Jiang G, Sutton DH, Critchley DR, Sheetz MP. Talin1 is critical for force-dependent reinforcement of initial integrin-cytoskeleton bonds but not tyrosine kinase activation. J Cell Biol 2003;163:409–19. [PubMed: 14581461]

Ginsberg MH, Partridge A, Shattil SJ. Integrin regulation. Curr Opin Cell Biol 2005;17:509–16. [PubMed: 16099636]

Gullberg D, Velling T, Lohikangas L, Tiger CF. Integrins during muscle development and in muscular dystrophies. Front Biosci 1998;3:D1039–50. [PubMed: 9778539]

Hamer PW, McGeachie JM, Davies MJ, Grounds MD. Evans Blue Dye as an in vivo marker of myofibre damage: optimising parameters for detecting initial myofibre membrane permeability. J Anat 2002;200:69–79. [PubMed: 11837252]

Hayashi YK, Chou FL, Engvall E, Ogawa M, Matsuda C, Hirabayashi S, Yokochi K, Ziober BL, Kramer RH, Kaufman SJ, et al. Mutations in the integrin alpha7 gene cause congenital myopathy. Nat Genet 1998;19:94–7. [PubMed: 9590299]

Hynes RO. Integrins: versatility, modulation, and signaling in cell adhesion. Cell 1992;69:11–25. [PubMed: 1555235]

Jiang G, Giannone G, Critchley DR, Fukumoto E, Sheetz MP. Two-piconewton slip bond between fibronectin and the cytoskeleton depends on talin. Nature 2003;424:334–7. [PubMed: 12867986]

Lee M, Cram EJ, Shen B, Schwarzbauer JE. Roles for beta(pat-3) integrins in development and function of Caenorhabditis elegans muscles and gonads. J Biol Chem 2001;276:36404–10. [PubMed: 11473126]

Leptin M, Bogaert T, Lehmann R, Wilcox M. The function of PS integrins during Drosophila embryogenesis. Cell 1989;56:401–8. [PubMed: 2492451]

Leu M, Bellmunt E, Schwander M, Farinas I, Brenner HR, Muller U. Erbb2 regulates neuromuscular synapse formation and is essential for muscle spindle development. Development 2003;130:2291–301. [PubMed: 12702645]

Li F, Zhang Y, Wu C. Integrin-linked kinase is localized to cell-matrix focal adhesions but not cell-cell adhesion sites and the focal adhesion localization of integrin-linked kinase is regulated by the PINCH-binding ANK repeats. J Cell Sci 1999;112(Pt 24):4589–99. [PubMed: 10574708]

Lieber RL, Woodburn TM, Friden J. Muscle damage induced by eccentric contractions of 25% strain. J Appl Physiol 1991;70:2498–507. [PubMed: 1885443]

Liu S, Calderwood DA, Ginsberg MH. Integrin cytoplasmic domain-binding proteins. J Cell Sci 2000;113 (Pt 20):3563–71. [PubMed: 11017872]

Livak KJ, Schmittgen TD. Analysis of relative gene expression data using real-time quantitative PCR and the 2(-Delta Delta C(T)) Method. Methods 2001;25:402–8. [PubMed: 11846609]

Mayer U, Saher G, Fassler R, Bornemann A, Echtermeyer F, von der Mark H, Miosge N, Poschl E, von der Mark K. Absence of integrin alpha 7 causes a novel form of muscular dystrophy. Nat Genet 1997;17:318–23. [PubMed: 9354797]

McCann RO, Craig SW. The I/LWEQ module: a conserved sequence that signifies F-actin binding in functionally diverse proteins from yeast to mammals. Proc Natl Acad Sci U S A 1997;94:5679–84. [PubMed: 9159132]

McCann RO, Craig SW. Functional genomic analysis reveals the utility of the I/LWEQ module as a predictor of protein:actin interaction. Biochem Biophys Res Commun 1999;266:135–40. [PubMed: 10581178]

McNeil PL, Khakee R. Disruptions of muscle fiber plasma membranes. Role in exercise-induced damage. Am J Pathol 1992;140:1097–109. [PubMed: 1374591]

Miosge N, Klenczar C, Herken R, Willem M, Mayer U. Organization of the myotendinous junction is dependent on the presence of alpha7beta1 integrin. Lab Invest 1999;79:1591–9. [PubMed: 10616209]

Mitra SK, Hanson DA, Schlaepfer DD. Focal adhesion kinase: in command and control of cell motility. Nat Rev Mol Cell Biol 2005;6:56–68. [PubMed: 15688067]

Monkley SJ, Pritchard CA, Critchley DR. Analysis of the mammalian talin2 gene TLN2. Biochem Biophys Res Commun 2001;286:880–5. [PubMed: 11527381]

Monkley SJ, Zhou XH, Kinston SJ, Giblett SM, Hemmings L, Priddle H, Brown JE, Pritchard CA, Critchley DR, Fassler R. Disruption of the talin gene arrests mouse development at the gastrulation stage. Dev Dyn 2000;219:560–74. [PubMed: 11084655]

Nieswandt B, Moser M, Pleines I, Varga-Szabo D, Monkley S, Critchley D, Fassler R. Loss of talin1 in platelets abrogates integrin activation, platelet aggregation, and thrombus formation in vitro and in vivo. J Exp Med 2007;204:3113–8. [PubMed: 18086864]

Petrich BG, Marchese P, Ruggeri ZM, Spiess S, Weichert RA, Ye F, Tiedt R, Skoda RC, Monkley SJ, Critchley DR, et al. Talin is required for integrin-mediated platelet function in hemostasis and thrombosis. J Exp Med 2007;204:3103–11. [PubMed: 18086863]

Riveline D, Zamir E, Balaban NQ, Schwarz US, Ishizaki T, Narumiya S, Kam Z, Geiger B, Bershadsky AD. Focal contacts as mechanosensors: externally applied local mechanical force induces growth of focal contacts by an mDia1-dependent and ROCK-independent mechanism. J Cell Biol 2001;153:1175–86. [PubMed: 11402062]

Rooney JE, Welser JV, Dechert MA, Flintoff-Dye NL, Kaufman SJ, Burkin DJ. Severe muscular dystrophy in mice that lack dystrophin and alpha7 integrin. J Cell Sci 2006;119:2185–95. [PubMed: 16684813]

Rosalki SB. Serum enzymes in disease of skeletal muscle. Clin Lab Med 1989;9:767–81. [PubMed: 2686911]

Sam M, Shah S, Friden J, Milner DJ, Capetanaki Y, Lieber RL. Desmin knockout muscles generate lower stress and are less vulnerable to injury compared with wild-type muscles. Am J Physiol Cell Physiol 2000;279:C1116–22. [PubMed: 11003592]

Schmalbruch H. Segmental fibre breakdown and defects of the plasmalemma in diseased human muscles. Acta Neuropathol (Berl) 1975;33:129–41. [PubMed: 1202896]

Schwander M, Leu M, Stumm M, Dorchies OM, Ruegg UT, Schittny J, Muller U. Beta1 integrins regulate myoblast fusion and sarcomere assembly. Dev Cell 2003;4:673–85. [PubMed: 12737803]

Schwenk F, Baron U, Rajewsky K. A cre-transgenic mouse strain for the ubiquitous deletion of loxP-flanked gene segments including deletion in germ cells. Nucleic Acids Res 1995;23:5080–1. [PubMed: 8559668]

Senetar MA, Foster SJ, McCann RO. Intrasteric inhibition mediates the interaction of the I/LWEQ module proteins Talin1, Talin2, Hip1, and Hip12 with actin. Biochemistry 2004;43:15418–28. [PubMed: 15581353]

Senetar MA, McCann RO. Gene duplication and functional divergence during evolution of the cytoskeletal linker protein talin. Gene 2005;362:141–52. [PubMed: 16216449]

Senetar MA, Moncman CL, McCann RO. Talin2 is induced during striated muscle differentiation and is targeted to stable adhesion complexes in mature muscle. Cell Motil Cytoskeleton 2007;64:157–73. [PubMed: 17183545]

Shi X, Garry DJ. Muscle stem cells in development, regeneration, and disease. Genes Dev 2006;20:1692–708. [PubMed: 16818602]

Sonnemann KJ, Fitzsimons DP, Patel JR, Liu Y, Schneider MF, Moss RL, Ervasti JM. Cytoplasmic gamma-actin is not required for skeletal muscle development but its absence leads to a progressive myopathy. Dev Cell 2006;11:387–97. [PubMed: 16950128]

Straub V, Rafael JA, Chamberlain JS, Campbell KP. Animal models for muscular dystrophy show different patterns of sarcolemmal disruption. J Cell Biol 1997;139:375–85. [PubMed: 9334342]

Taverna D, Disatnik MH, Rayburn H, Bronson RT, Yang J, Rando TA, Hynes RO. Dystrophic muscle in mice chimeric for expression of alpha5 integrin. J Cell Biol 1998;143:849–59. [PubMed: 9813102]

Tidball JG, O'Halloran T, Burridge K. Talin at myotendinous junctions. J Cell Biol 1986;103:1465–72. [PubMed: 3095335]

Vilquin JT, Brussee V, Asselin I, Kinoshita I, Gingras M, Tremblay JP. Evidence of mdx mouse skeletal muscle fragility in vivo by eccentric running exercise. Muscle Nerve 1998;21:567–76. [PubMed: 9572235]

Volk T, Fessler LI, Fessler JH. A role for integrin in the formation of sarcomeric cytoarchitecture. Cell 1990;63:525–36. [PubMed: 2225065]

Weller B, Karpati G, Carpenter S. Dystrophin-deficient mdx muscle fibers are preferentially vulnerable to necrosis induced by experimental lengthening contractions. J Neurol Sci 1990;100:9–13. [PubMed: 2089145]

Ziegler WH, Liddington RC, Critchley DR. The structure and regulation of vinculin. Trends Cell Biol 2006;16:453–60. [PubMed: 16893648]

Supplementary Material

Refer to Web version on PubMed Central for supplementary material.

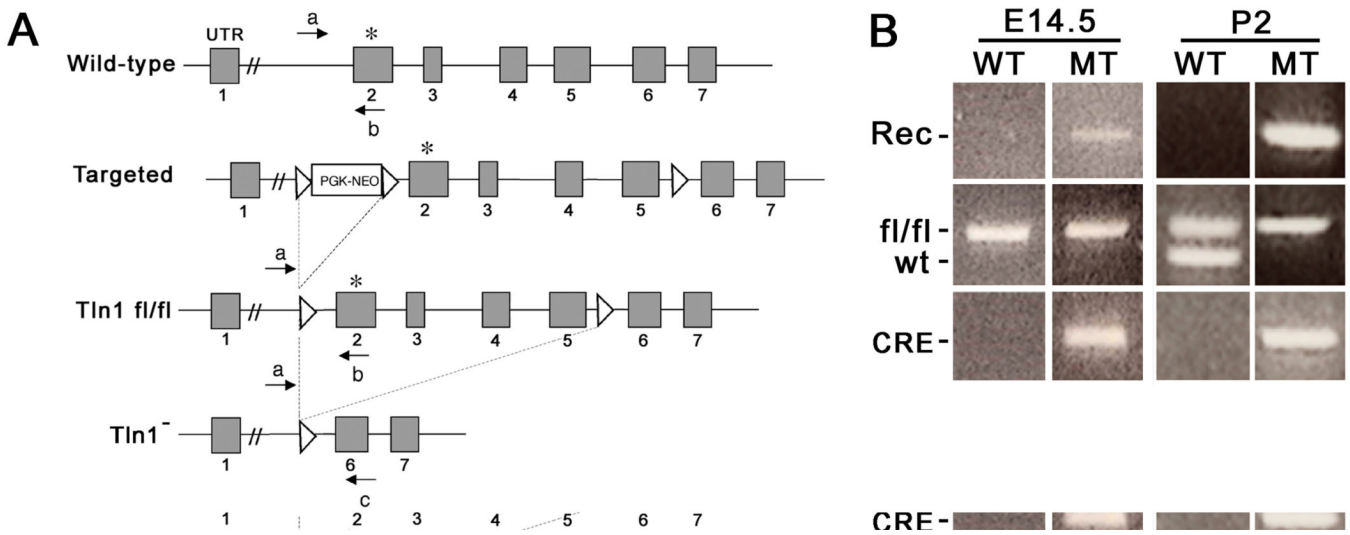

Figure 1. Generation of the talin 1 conditional allele

(A) Scheme of the targeting strategy. Homologous recombination of the targeting construct into the *Tln1* gene introduced a loxP site (triangle) downstream of coding exon 5 and a floxed *pgk-neo* cassette upstream of the first coding exon (exon 2). CRE expression induced three recombination events. Type II deletion: removal of the Neo cassette (Tln1 fl/fl); Type III deletion: removal of exons 1−4 (not shown); Type I deletion: removal of *pgk-neo* and exons 1−4 (Tln1⁻). a-c denote primers for PCR reactions shown in (B). (B) Recombination pattern observed by PCR on DNA extracted from E14.5 and P2 wild-type (WT) and mutant (MT) littermates. Upper panel: A 707 bp band indicative of the recombined allele (Rec) was observed in samples from *Tln1HSA-CREko* mice. Middle panel: the presence of floxed (fl) and wild type (wt) alleles was confirmed; Lower panel: the presence of CRE recombinase (CRE) was confirmed.

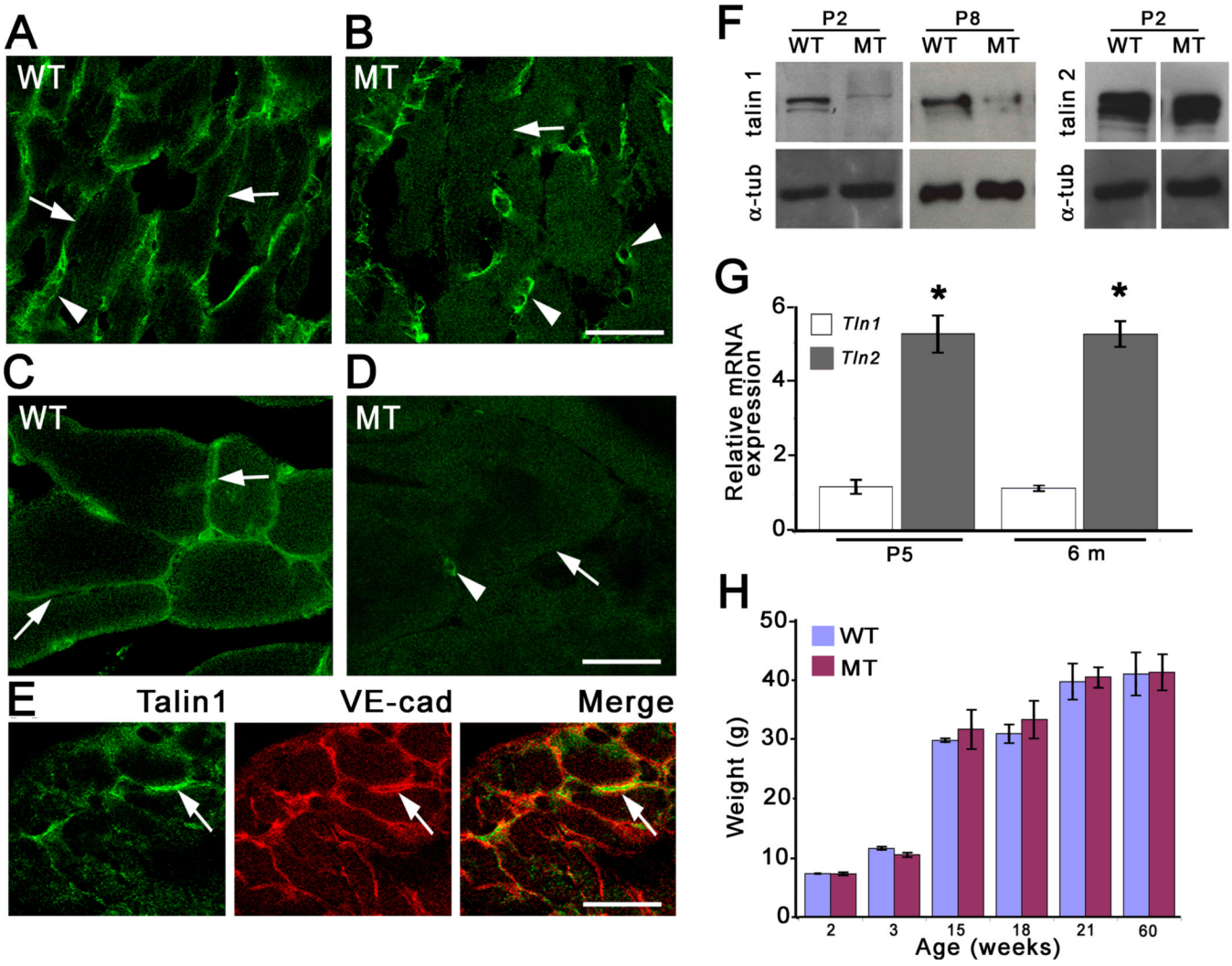

Figure 2. Characterization of *Tln1HSA-CREko* mice

(A-E) Cross sections of wild-type and mutant muscle were stained with antibodies to talin 1 at P8 (A, B) and 6 months (C, D). Talin 1 expression was detected at the sarcolemma in wild-type (A, C) but not mutant mice (B, D). In the mutants, talin 1 expression remained in cells between skeletal muscle fibres (B, D; arrowheads) that were identified as blood vessels by staining with antibodies to VE-cadherin (E). (F) Western blots with extracts from P2 and P8 gastrocnemius and soleus muscle, respectively. Expression of talin 1 was markedly reduced in *Tln1HSA-CREko* mice. Residual protein levels were likely due to talin 1 expression in endothelial cells. Talin 2 expression was detected in muscle extracts, but no compensatory upregulation was evident. Membranes were probed for tubulin as a loading control. (G) Analysis of *Tln1* and *Tln2* transcript levels in gastrocnemius muscle by quantitative real-time PCR. Data are plotted as relative to the *Tln1* mRNA levels (n=3; mean ± S.E). (H) Growth curve of wild-type (WT) and *Tln1HSA-CREko* (MT) mice up to 60 weeks of age revealed no differences between genotypes. Scale bars: (A-D) 25 μm; (E) 50 μm.

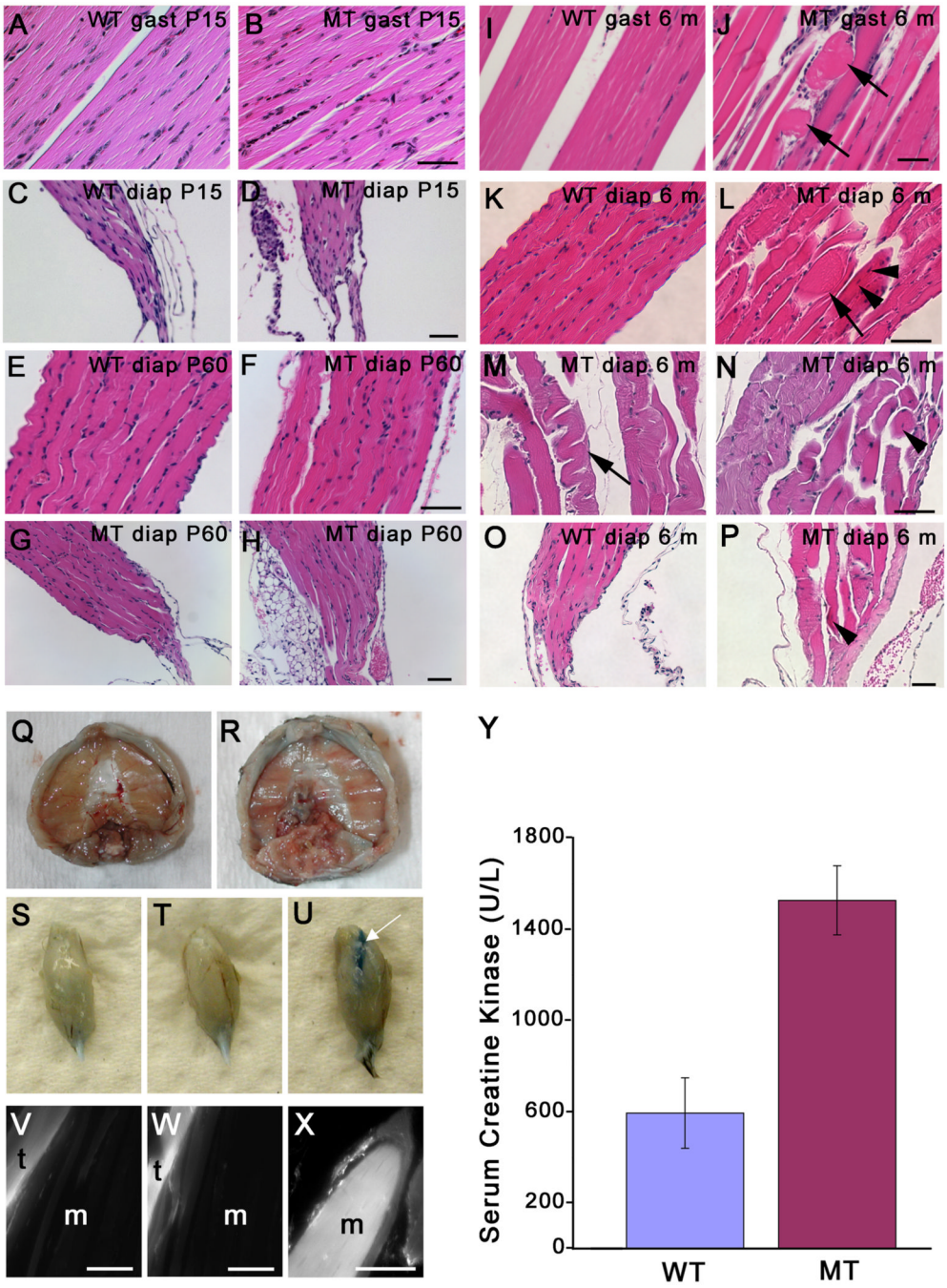

Figure 3. Skeletal muscle defects in *Tln1HSA-CREko* mice

(A-P) Muscle sections from wild-type and mutant animals were stained with hematoxylin and eosin. Longitudinal sections from gastrocnemius and diaphragm muscles at P15 (A-D) and P60 (E-H) revealed no defects in the mutants. At 6 months, defects were observed in gastrocnemius and diaphragm muscles in mutants (J, L-N, P), but not in wild types (I, K, O). Pathological changes included enlarged (J, L; arrows) and bent (M; arrow) muscle fibres, and centrally located nuclei (L, N, arrowheads). Abnormal muscle fibre morphology was also evident in proximity to MTJs (compare O, P). (Q-X) 6-months old mice were injected with EBD and analyzed for dye uptake via bright field illumination of whole mount tissue. Wild-type diaphragm (Q) and gastrocnemius muscle (S) did not show dye uptake, unless the muscle

fibres were damaged (U) (damage was occasionally observed in wild-type and mutant mice). No dye was incorporated in mutant fibres (R, T). (V-X) Dye uptake was analyzed in sections using immunofluorescence microscopy. Tendon (t) but not muscle (m) in wild-type (V) and mutants (W) had incorporated dye. In control damaged muscle from wild types (X), dye uptake was observed. (Y) At 6 months of age, mild increase in serum CK levels were observed in the mutants ($n \geq 4$; mean ± S.E). Scale bars: (A-P) 250 μm; (V-X) 200 μm.

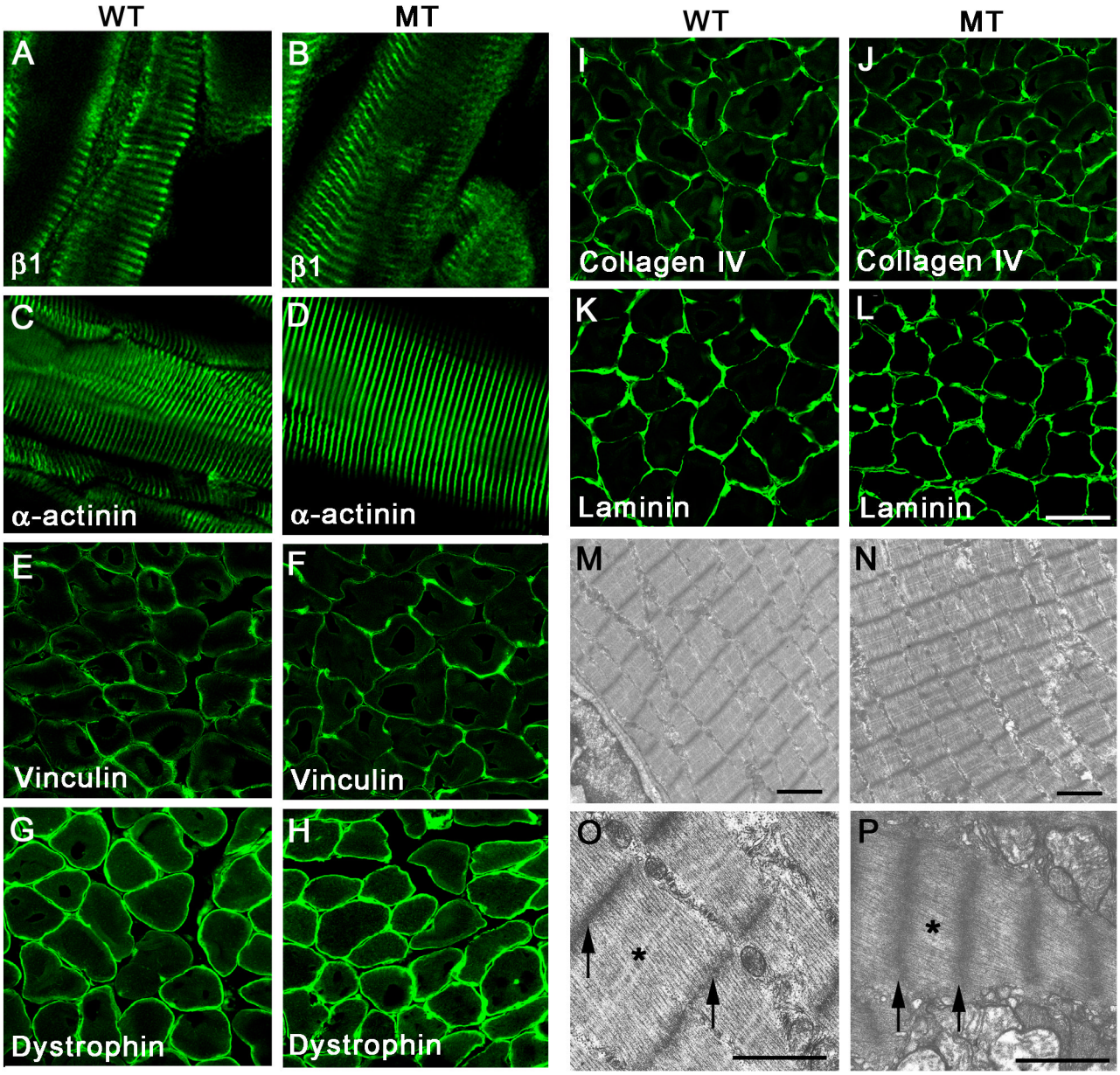

Figure 4. Talin 1 is not essential for costamere assembly

(A-D) Longitudinal and (EL) cross-sections of muscle from 6-months old wild-type and *Tln1HSA-CREko* mice were stained with antibodies to costameric proteins and ECM glycoproteins and analyzed by immunofluorescence microscopy. The integrin β1-subunit, α-actinin, vinculin, dystrophin, collagen type IV and laminin were normally localized in the mutants. (M-P) Analysis of muscle by transmission electron microscopy. Sarcomere organization was not affected in *Tln1HSA-CREko* mice (M,N), but sarcomeres occasionally appeared hypercontracted (O,P). The Z-band was always detectable (O,P, arrows), but the A band (O,P, asterisk) was sometimes not evident in contracted muscle fibres. Scale bars: (A-L) 200 μm; (M,N), 2 μM; (O,P) 1 μm.

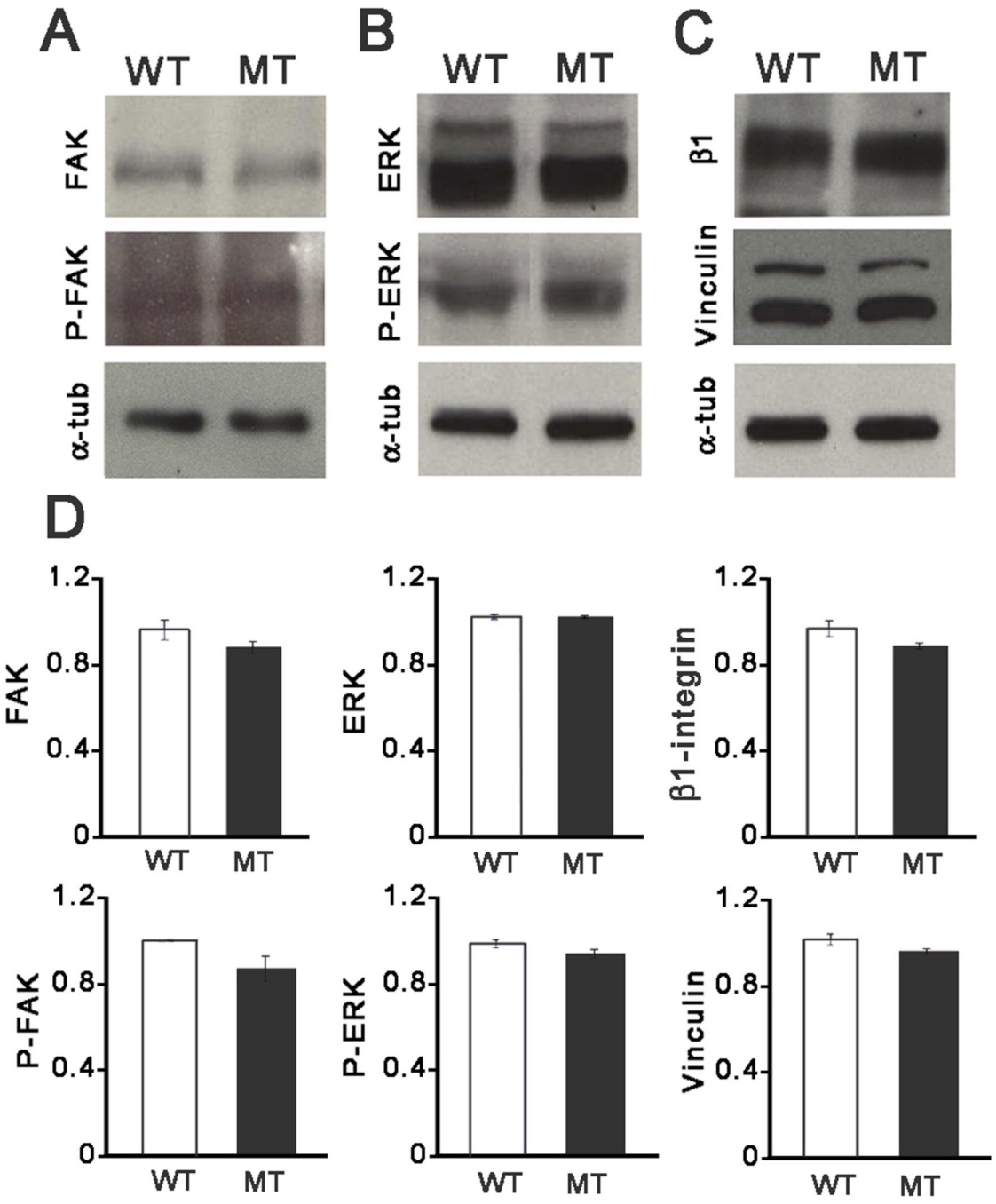

Figure 5. Expression and phosphorylation of talin 1-associated proteins

(A-C) Extracts from gastrocnemius muscles were analyzed by Western blotting. No changes were observed in levels of FAK (A), ERK1/2 (B), β1-integrin and vinculin (C). Phosphorylation of FAK at Tyr^{397} (A), and ERK 1/2 (B) were unaffected. Membranes were probed with α-tubulin antibodies as a loading control. (D) Protein expression was quantified by densitometry ($n \geq 3$; relative expression levels ± S.E.). No statistically significant expression difference was observed (p-values: β1-integrin = 0.238; vinculin = 0.146; FAK = 0.223; P-FAK = 0.153; ERK1/2 = 0.892; P-ERK1/2 = 0.165).

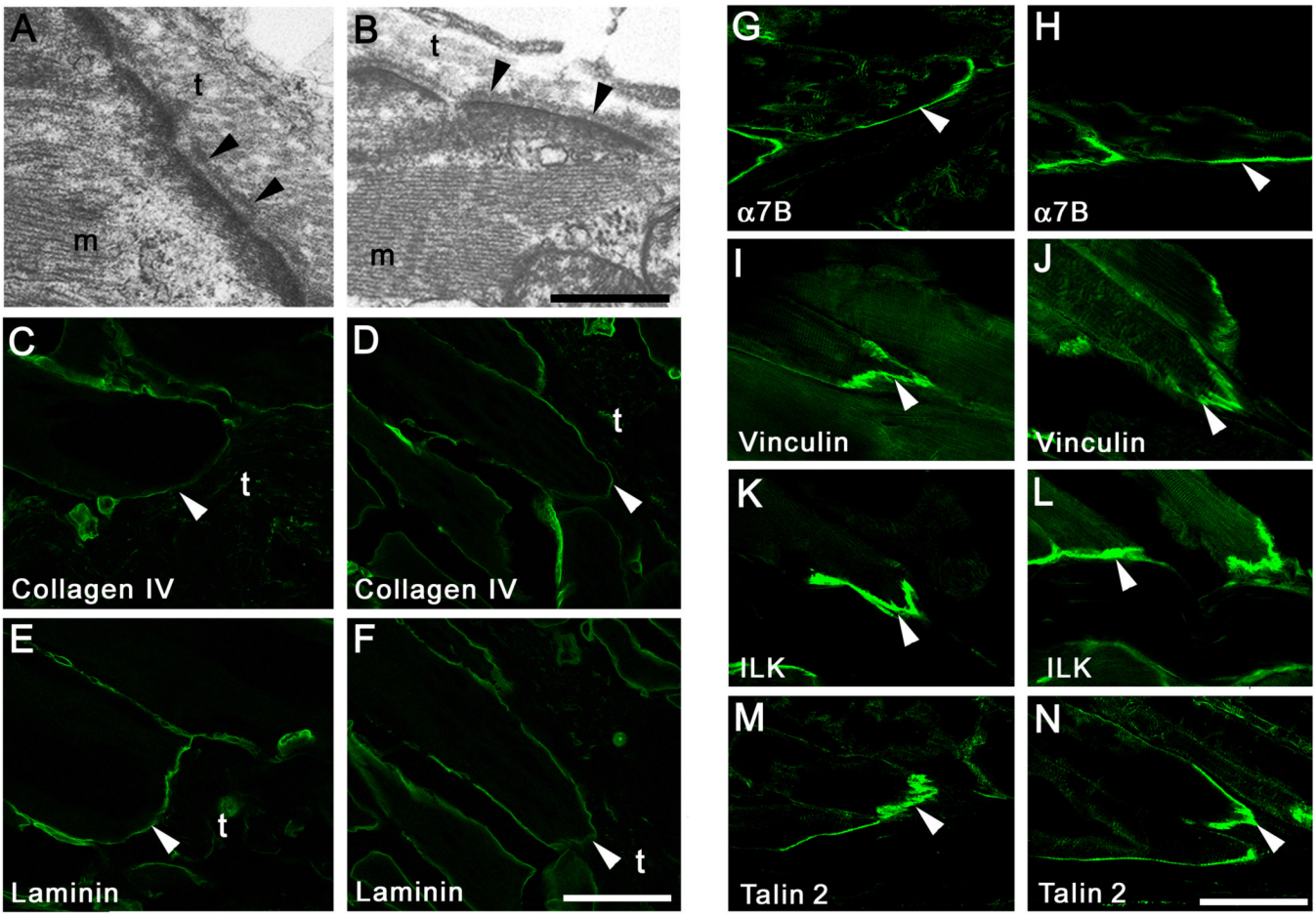

Figure 6. Integrin complexes are maintained at MTJ

(A,B) MTJs in diaphragm muscle from wild-type and mutant animals were analyzed by transmission electron microscopy to reveal the lamina densa. A continuous basement membrane (arrowheads) was present at the MTJ in mutants; t, tendon, m, muscle. (C-N) Localization of proteins to MTJs (arrows) was analyzed by immunofluorescence microscopy. All analyzed proteins were present at MTJs in wild-type and mutant animals. Scale bars: (A,B) 500 nm; (C-F) 100 μm; (G-N) 200 μm.

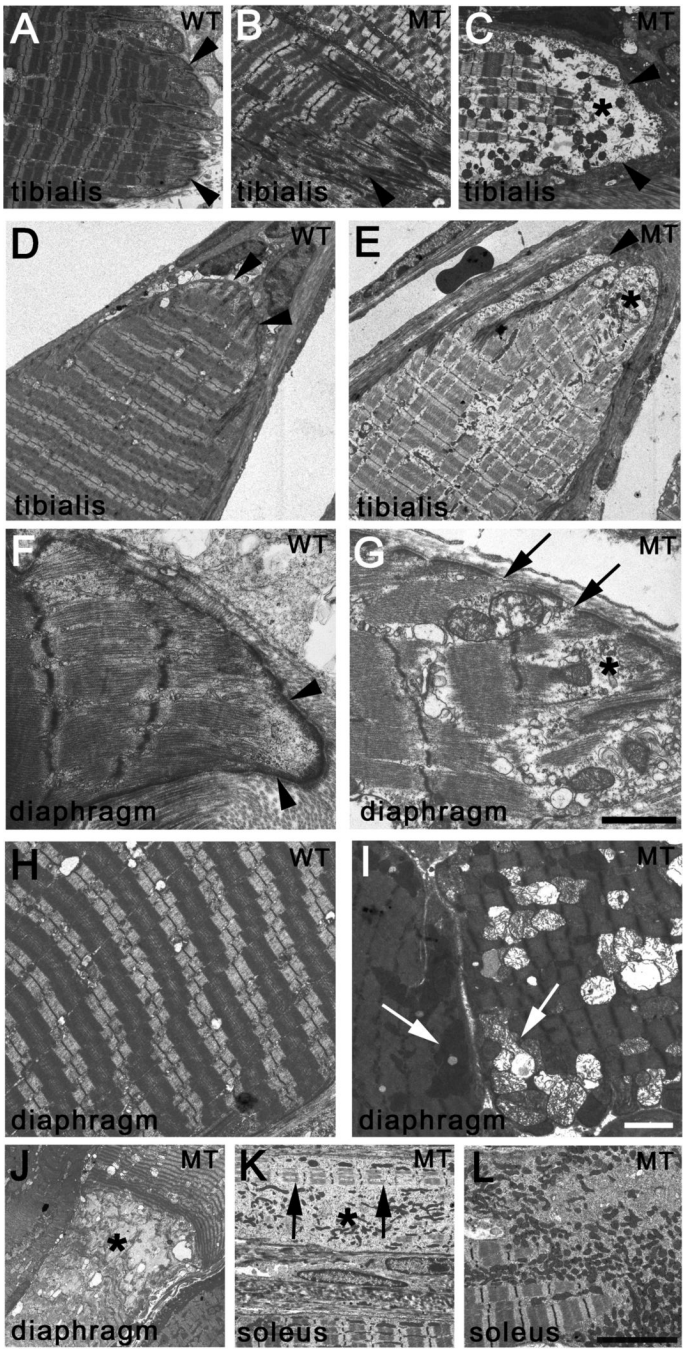

Figure 7. Detachment of myofilaments at the MTJ

Electron micrographs of tibialis (A-E), diaphragm (F-J) and soleus (K,L) muscles collected from 1-month (A-C, H, I) and 6- month-old (D-G, J-L) mice. In wild-type mice, myofilaments connected to junctional electron-dense plaques are visible (arrowheads in A, D, F). In 1-month old *Tln1HSA-CREko* mice, most MTJ were intact (B), but detachment of myofibres from MTJs was occasionally observed (C). In 6-months old mutant animals, detachment of the myofibres was observed very frequently (E). Necrotic material was present where myofibres detached (asterisks in C, E, G). The thickness of the junctional plaque was reduced, and gaps were present where myofilaments failed to attach (arrows in G). Degeneration (I) and accumulation (K, L) of mitochondria was observed. Necrotic areas were observed in mutant fibres (J, K; asterisk)

next to abnormal myofilaments (K; arrows). Scale bars: (AE,H,I) 3 μm; (F,G) 1 μm; (J-L) 10 μm.

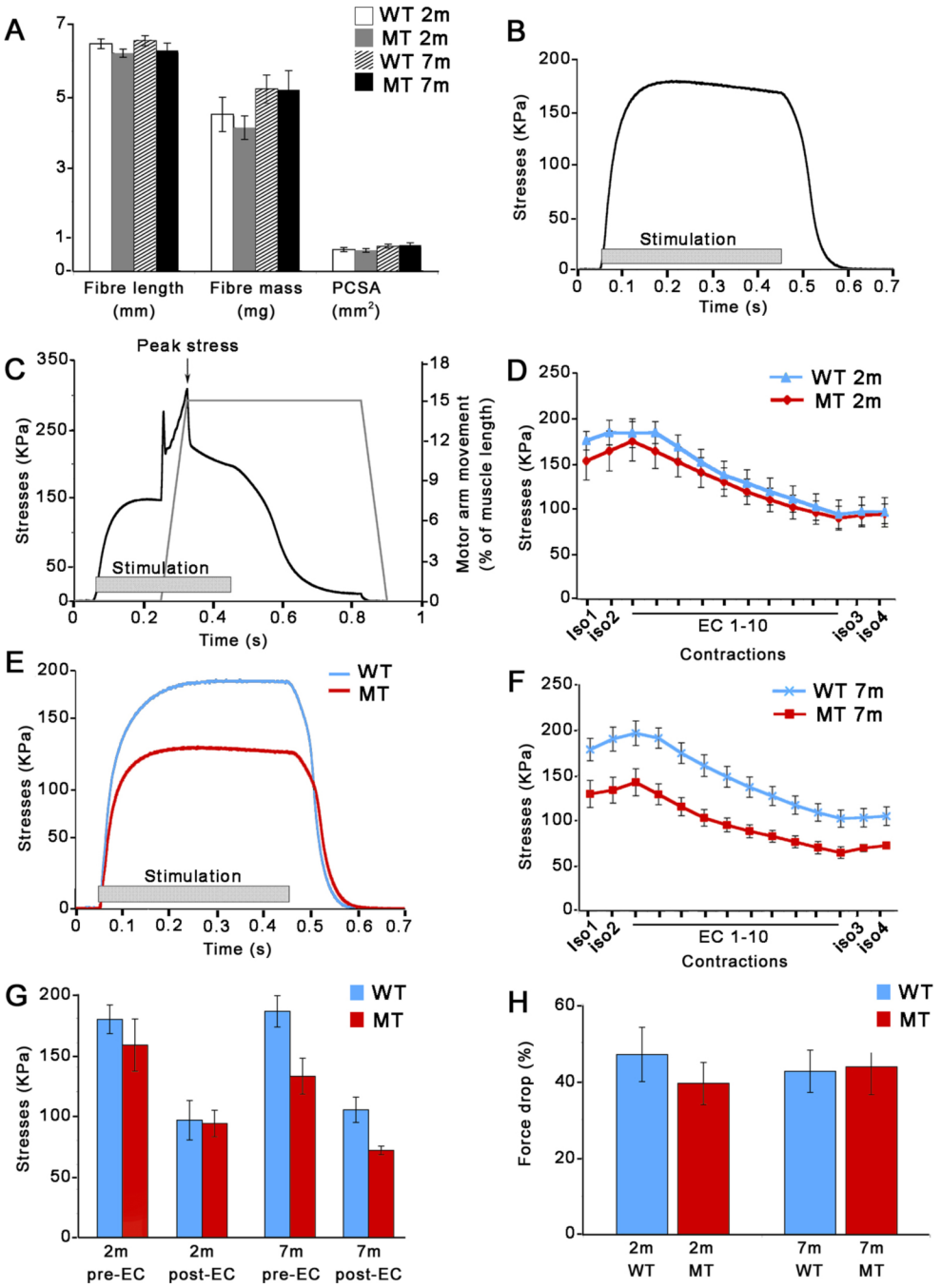

Figure 8. Impaired force generation by Tln1-deficient muscles

(A) The length, mass and physiological cross-sectional area (PCSA) are similar in the 5th EDL muscle from wild-type and *Tln1HSA-CREko* mice. (B, C) Sample curves representing a single isometric and eccentric contraction, respectively. (D-H) Isometric and eccentric contractile properties of the 5th EDL muscle isolated from 2- and 7-month-old mice. (D) No significant difference was observed in stress exerted by 2-months old muscles from wild-type and *Tln1HSA-CREko* mice in the eccentric contraction protocol. (E) Example of force profile of the first isometric contraction in 7 months old mice. *Tln1*-deficient muscles exert reduced isometric stress. (F, G) In an eccentric contraction protocol, muscles from 7-month old *Tln1HSA-CREko* mice showed a significant reduction in peak stress exerted in the pre-eccentric

(p=0.0276) and post-eccentric (p=0.0358) isometric contractions compared to wild-type controls ($n \geq 4$ per genotype/time point). (H) Even though *Tln1*-deficient muscles generated less force than controls, the force drop was comparable between genotypes, suggesting enhanced susceptibility to damage in the mutants. All force values were normalised against the PCSA of muscle (means ± S.E.).